

# Image-based bidirectional reflectance distribution function measurement

Stephen R. Marschner, Stephen H. Westin, Eric P. F. Lafortune, and Kenneth E. Torrance

We present a new image-based process for measuring a surface's bidirectional reflectance rapidly, completely, and accurately. Requiring only two cameras, a light source, and a test sample of known shape, our method generates densely spaced samples covering a large domain of illumination and reflection directions. We verified our measurements both by tests of internal consistency and by comparison against measurements made with a gonireflectometer. The resulting data show accuracy rivaling that of custom-built dedicated instruments. © 2000 Optical Society of America

OCIS codes: 290.5820, 120.5820, 160.4760, 290.5880, 110.2960.

## 1. Introduction

One of the major goals of computer graphics is to synthesize realistic images of scenes modeled in a computer. To create such a realistic image, a complete model or description of reflectance is needed for each reflective surface in the scene. In optics terminology, the complete bidirectional reflectance distribution function (BRDF) described by Nicodemus *et al.*<sup>1</sup> is needed. In contrast to many optical inspection and surface metrology applications, computer rendering requires BRDF information over the complete scattering hemisphere for any incident direction, including wavelength-dependent information for color. Computer graphics has long been aware of the BRDF literature, beginning with Blinn's<sup>2</sup> adaptation of the work of Torrance and Sparrow,<sup>3</sup> but physically based models are still used only occasionally, both because of their complexity and because parameters are not readily available. Rendering from measured BRDF data is also possible,<sup>4</sup> but even rarer because the necessary BRDF data are not widely available.

---

When this research was undertaken, S. R. Marschner, S. H. Westin (shw5@cornell.edu), E. P. F. Lafortune, and K. E. Torrance (ket1@cornell.edu) were with the Program of Computer Graphics, Cornell University, 580 Rhodes Hall, Ithaca, New York 14853-3801. S. R. Marschner (stevemar@microsoft.com) is now with Microsoft Research, One Microsoft Way, Redmond, Washington 98052-6399. E. P. F. Lafortune (Eric.Lafortune@luciad.com) is now with Luciad, Parijsstraat 74, Leuven B-3000 Belgium.

Received 7 October 1999.

0003-6935/00/162592-09\$15.00/0

© 2000 Optical Society of America

Several researchers have built BRDF measurement instruments specifically for computer graphics. Some have used custom-made equipment; others have measured only a small part of the hemisphere to supply data for fitting the parameters of a simple BRDF model. None has stressed absolute accuracy, instead aiming for visually plausible reflectances.

In this paper we present a system that measures reflectance quickly, completely, and without special equipment. The method works by our taking a series of photographs of a curved object. Each image captures light reflected from many differently oriented parts of the surface, and with the knowledge of the sample shape and the light source position the photographs can be analyzed to determine the sample's BRDF. By using a curved test sample and an imaging detector, we eliminate the mechanism needed to position the detector in a traditional gonireflectometer; and by using automated photogrammetry to measure the source position, we eliminate the precise source positioning mechanism. Although the apparatus is simple and the measurement is rapid, the technique provides millions of accurate samples that cover the full hemisphere to angles near grazing.

## 2. Prior Research

The BRDF is measured traditionally with a gonireflectometer, positioning a source and detector with respect to a flat sample. Four degrees of rotational freedom are needed, because, apart from wavelength, the BRDF is a function of four variables: two for the illumination direction and two for the reflection direction. For isotropic surfaces—those whose BRDF

is invariant under rotation about the surface normal—the BRDF has just three angular variables, requiring three geometric degrees of freedom. In this paper we concentrate on this important class of materials.

We denote the incident and exitant directions by  $(\theta_i, \phi_i)$  and  $(\theta_e, \phi_e)$ , with  $\theta$  measuring elevation ( $\theta = 0$  at the surface normal) and  $\phi$  measuring azimuth. An isotropic BRDF depends only on the difference in azimuth,  $\Delta\phi = \phi_e - \phi_i$ , so the variables  $\theta_i$ ,  $\theta_e$ , and  $\Delta\phi$  suffice in the isotropic case.

In a classical setup,<sup>5,6</sup> the three or four angular dimensions are handled by specialized mechanisms that position a light source and a detector at various directions from a flat sample of the material to be measured. The final dimension, that of wavelength, is handled either with a broadband spectroradiometer that measures the entire spectrum at once or by multiple measurements varying the wavelength of a narrow-band source or detector. Because three, four, or five dimensions must be sampled sequentially, the measurement of reflectance functions can be time-consuming, even with modern computer controls. Moving the motor stages and measuring the reflected light can take several seconds, and, because measurements are taken point by point, even a sparse sampling of the incident and exitant hemispheres can take several hours.

The advent of good two-dimensional (2-D) image sensor arrays, such as CCD's, offers the opportunity to reduce dimensionality in angle rather than in wavelength. The sensor array can measure a 2-D range of angles simultaneously, leaving one or two dimensions of angle and one dimension of wavelength to be sampled by sequential measurements.

Several such instruments have been developed to measure scattering for optical inspection and metrology purposes. They typically simplify BRDF measurement by any (or several) of the following restrictions: covering a subset of the scattering hemisphere, using a single incident direction, or measuring at a single wavelength. Breault Research's OmniScatR device<sup>7</sup> uses fiber optics to collect multiple points on the hemisphere and direct them to a CCD array. It covers a  $44^\circ$  cone of the scattering hemisphere in one measurement. Hatab *et al.*<sup>8</sup> and McNeil and Wilson<sup>9</sup> built a device that uses a hemispherical screen to capture scattered laser light; this screen is imaged onto a CCD array. Davis and Rawlings<sup>10</sup> at Boeing have recently patented a device using an ellipsoidal mirror to gather a large part of the scattering hemisphere onto a CCD sensor.

Computer graphics, however, demands both full hemispherical BRDF information and complete coverage of the visible spectrum. Exhaustive measurement of the entire hemispheres of the BRDF is required because image synthesis algorithms must evaluate the BRDF in arbitrary directions. The visible wavelength spectrum must be covered for correct color reproduction. On the other hand, accuracy within a few percent is quite acceptable, only visible

wavelengths are of interest, and coarse wavelength resolution is often sufficient.

Computer graphics practitioners need complete data, but usually lack the resources of an optical measurement laboratory. It is important to use relatively nonspecialized equipment in a relatively simple procedure. Because of these demands, researchers in computer graphics have developed techniques and instruments specifically to acquire the data needed.

Ward<sup>4</sup> used a curved mirror to gather light scattered from a flat sample into a CCD camera with a fish-eye lens. By use of a semisilvered mirror, the camera captures the entire exitant hemisphere at once for each illumination direction, leaving 2 degrees of freedom to handle mechanically. Ward's instrument is limited by its optics; the hemispherical mirror only approximates the ideal ellipsoid used later by Davis and Rawlings, and vignetting limits the quality of measurements near grazing exitance. Ward used the red-green-blue (RGB) filters of his CCD camera to yield three bands of spectral information.

Ikeuchi and Sato<sup>11</sup> present a system for estimating reflectance model parameters using a surface model from a range scanner and a single image from a video camera. In contrast to Ward's method, they use a curved sample to capture a set of directions spanning a large range of both incident and exitant directions. Because their goal is to fit a reflectance model, they use a single image and make no attempt to sample the BRDF exhaustively.

More recently, Lu *et al.*<sup>12</sup> use photographs of a cylindrical sample to give broad angular coverage in the incidence plane, using multiple images with different source positions to cover all angles. Their goals and methods are similar to ours for the special case of incidence-plane measurements. However, we present measurements for the full isotropic BRDF, and we verified the accuracy of our results.

Our method improves on this previous research by measuring isotropic BRDF's completely and accurately, while retaining simplicity, speed, and sampling density. Our results can be used not only to render images, but also to validate reflectance models for particular materials or to investigate BRDF's that do not conform to existing models.

In the following sections we describe the specifics of our system, give the results of measuring several materials, and demonstrate the accuracy of these results by comparing them with measurements from a gonioreflectometer.

### 3. Method

#### A. Measurement Setup and Technique

Our system, pictured in Fig. 1, uses digital photographs to record light reflected from the surface of a test sample of known shape and unknown but uniform BRDF. It measures the three dimensions of an isotropic BRDF by using the curvature of the surface to vary two of the three angles and a sequence of

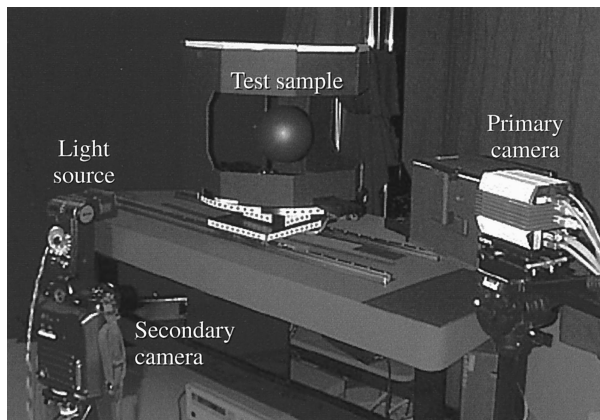


Fig. 1. Measurement setup.

photographs to vary the third. To do this, we illuminate the sample from a sequence of known positions, using a fixed primary camera to take a photograph for each position (Fig. 2). The pixels in each of the resulting images give measurements of light reflected from various points on the surface; the known geometry of the surface, light source, and camera allows the incident and exitant directions to be computed for each pixel. Each pixel in each image thus provides a measurement of the BRDF for a particular configuration of incident and exitant directions. Depending on the sample geometry, we may obtain several independent measurements for each configuration, which can be compared to verify the measurement or averaged to reduce random errors.

We can completely measure the BRDF in the plane of incidence by using a cylindrical sample. Because the sample's curvature lies along a single direction, we can arrange for the light source, camera, and surface normal always to lie in a plane. Each image will give measurements along a range of  $(\theta_i, \theta_e)$  pairs, with  $\Delta\phi = 0$  (Fig. 3). A set of these images, each acquired with the light source in a different position, produces a family of such curves, which together fill the entire 2-D parameter space of the incidence-plane BRDF. We move the light source along a path from near the camera (where we measure near retroreflection) to opposite the camera (where we measure grazing-angle reflection).

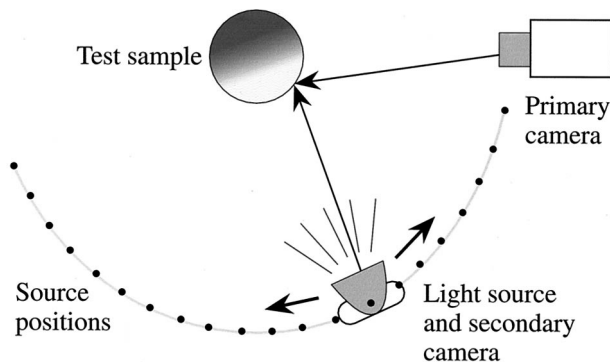


Fig. 2. Schematic of the measurement setup.

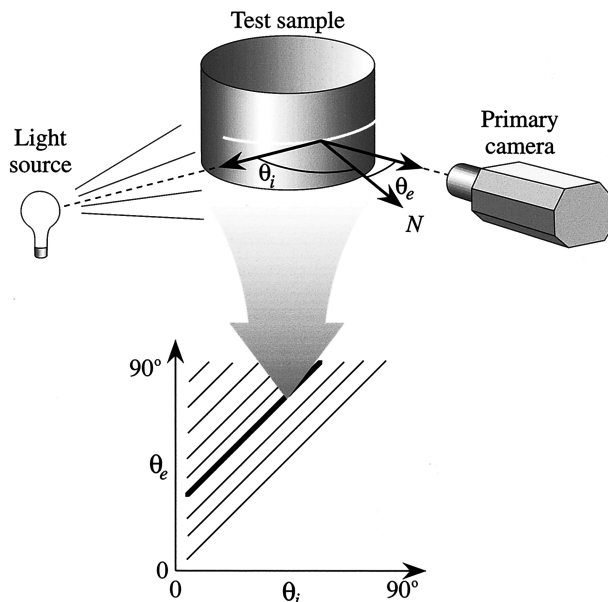


Fig. 3. Mapping from the surface to the BRDF parameter space in the incidence plane. If both camera and source were at an infinite distance from the sample,  $\theta_e - \theta_i$  would be constant and the diagonal lines would be straight as shown; in our measurements, they are slightly curved.

To measure the BRDF over the complete hemisphere for an isotropic surface, we use a spherical sample, which has curvature in both directions. In this case, the same set of light source positions leads to measurements on a family of 2-D surfaces of  $(\theta_i, \theta_e, \Delta\phi)$  triples, which together fill the three-dimensional (3-D) parameter space of the isotropic BRDF.

#### B. Apparatus

Our photographic BRDF measurement technique requires a well-characterized camera, a stable and uniform light source, and a means for measuring their positions. Also required are curved samples of accurately known shape.

Our system comprises the following parts:

- the primary camera: a cooled 12-bit CCD still camera (Photometrics PXL 1300L);
- the light source: a consumer electronic flash powered by a regulated dc power supply (Nikon SB-16 and HP 6030A);
- a secondary CCD camera for position measurement (Kodak DCS 420); and
- the samples: metal spheres painted with various sprayed coatings and metal cylinders painted similarly or wrapped with sheets of flexible material.

The primary camera, which remains fixed, makes the actual measurements of radiance reflected from the test sample. We adjust its overall sensitivity using neutral-density filters as appropriate to allow measurement of bright reflections without clipping. If a wavelength-dependent measurement is required,

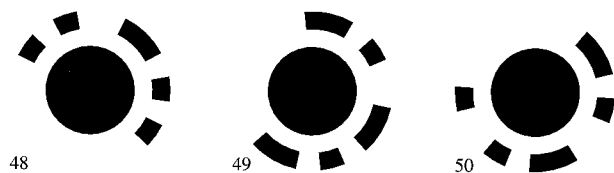


Fig. 4. Examples of photogrammetric targets.

we make sequential exposures using color separation filters.

We attach the secondary camera to the light source to measure the position of the source using automatic photogrammetry. Each measurement exposure is made by our opening the shutter of the primary camera, then triggering the secondary camera during the exposure. The secondary camera triggers the flash, so we obtain a calibration image directly correlated with the source position, acquired at exactly the same time as the measurement image. Each calibration image includes a field of machine-readable targets with known 3-D positions relative to the test sample and the primary camera. These targets are visible in Fig. 1, below the test sample, and actual-size examples are shown in Fig. 4. By analyzing these images, we can automatically determine the poses of the secondary camera. Both an *a priori* error estimate and residuals from the fitting processes involved (see Subsection 3.D) confirm that these poses are accurate to within a few millimeters. With the light source rigidly attached to the camera, its position is easily found for each exposure.

Because we measure the light source position in this way, the light source can be placed freely; the light source and secondary camera are placed on a tripod and moved manually from one position to the next over the course of the measurement. We typically use 32 light source positions ranging from 1.3 to 2.5 m from the sample.

### C. Calibration

To interpret a pixel value as a measurement of BRDF, the following must be known:

- the responsivity of the pixel sensor to scene radiance;
- the irradiance due to the light source at the relevant surface point; and
- the geometric arrangement of the surface normal, the viewing direction, and the illumination direction.

We undertook several calibration steps to ensure that each of these items was well controlled.

Because our primary camera uses a CCD array (Kodak KAF-1300i, serial no. MA-3254, chilled to  $-25^{\circ}\text{C}$ ), we expect that the response of each CCD element is directly proportional to scene radiance.<sup>13,14</sup> This was confirmed experimentally for our camera.<sup>15</sup> Physical variation between sensors and limitations of the lens optics cause a variation in the constant of proportionality across the image. We measured this

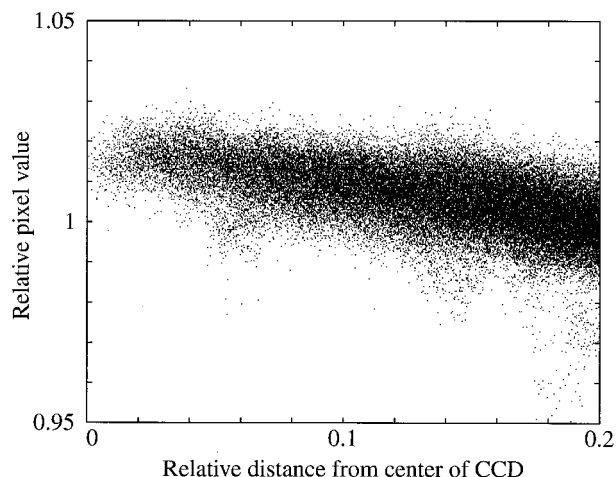


Fig. 5. Field flatness of camera: normalized pixel response versus radius for image area used.

nonuniformity by imaging the exit port of an integrating sphere (Labsphere CSTM-USS-1200). The variation over the entire image plane was of the order of 10%, but we used only the central portion where variation was limited to within 2% of uniform, as shown in Fig. 5.

We modeled our source as a point with uniform angular distribution. To confirm this, we measured the angular variation of the source by photographing a white surface illuminated by the flash; this showed the irradiance to be uniform to within  $\pm 3\%$  over the  $\pm 5^{\circ}$  range of angles we use, as shown by the contour plot in Fig. 6. We reduced the variation from flash to flash, shown in Fig. 7, to less than 1% from the mean by replacing the flash's battery pack with a regulated voltage. We also verified that the flash's output was essentially unpolarized.

These steps allow radiance and irradiance to be determined in relative units, but we still need to establish a global scale factor to compute the absolute BRDF. We measured this factor by illuminating a

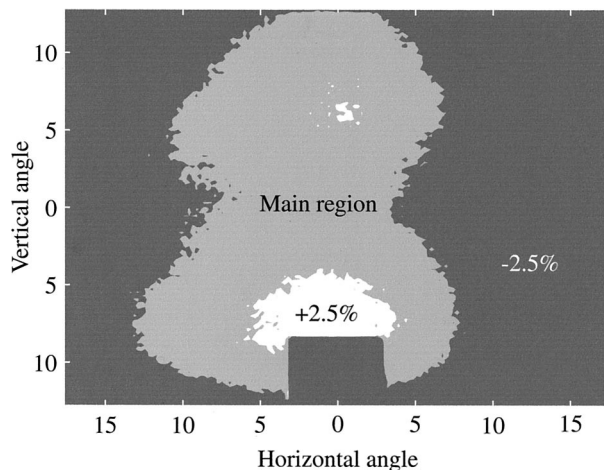


Fig. 6. Contour plot of relative flash irradiance: contour lines at  $\pm 2.5\%$  mean irradiance of center region.

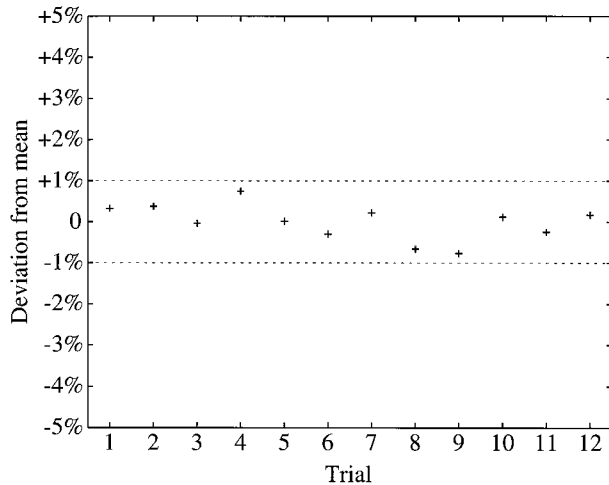


Fig. 7. Repeatability of flash with 30-s cycle time.

calibrated diffuse reference sample (Spectralon SRS-99-010, calibrated by Labsphere in Report 14424-A) in a known geometry and measuring the camera signal through each of the color filters. All BRDF measurements were then relative to the known BRDF of the calibration sample.

The final prerequisite to BRDF measurement is to know the incident and exitant directions. To calculate these, we must know the positions of the light source, test sample, and camera. Any errors in the direction to the camera or light source will cause errors in the calculated angles corresponding to each pixel; also, every 1% error in light source distance leads to a 2% error in the estimated irradiance. To establish the positions of the targets used to measure the location of the light source (see Subsection 3.B), we used the secondary camera and the photogrammetric technique of self-calibrating bundle adjustment.<sup>16,17</sup> This determines the targets' positions to submillimeter precision, as estimated from residual errors in the least-squares fit.

We estimate the solid angle of our detector from the  $f$ -number of the lens, ranging from  $f:11$  to  $f:22$  in these measurements, and the distance from detector to sample, which was 1.3 m. From the nominal 28-mm focal length of the lens, we can calculate

$$\begin{aligned} \Omega_{\min} &= \pi \left( \frac{0.028}{22} \right)^2 \\ &= 3.0 \times 10^{-6} \text{ sr}, \end{aligned} \quad (1)$$

$$\begin{aligned} \Omega_{\max} &= \pi \left( \frac{0.028}{11} \right)^2 \\ &= 1.2 \times 10^{-5} \text{ sr}. \end{aligned} \quad (2)$$

The effective solid angle of the source is somewhat harder to estimate, both because of the varying distance from the sample and because its output is not

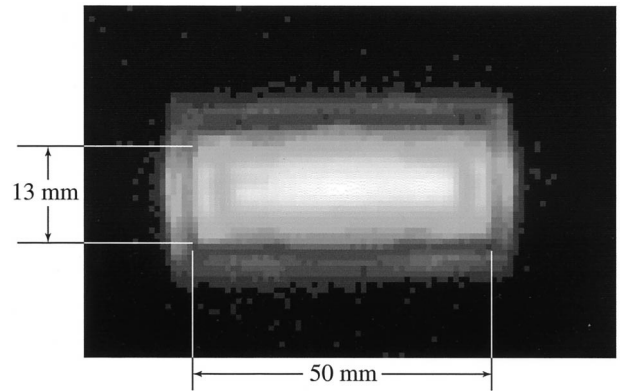


Fig. 8. Radiance across face of flash (nonlinear mapping).

evenly distributed across its face. Measurements based on an image of the front of the flash (Fig. 8) suggest that it has an effective radiating surface of 50 mm  $\times$  13 mm. From the maximum (2.6-m) and minimum (1.3-m) distances used in the measurements, we can calculate

$$\begin{aligned} \Omega_{\min} &= \pi \frac{0.050 \times 0.013}{2.6^2} \\ &= 3.0 \times 10^{-4} \text{ sr}, \end{aligned} \quad (3)$$

$$\begin{aligned} \Omega_{\max} &= \pi \frac{0.050 \times 0.013}{1.3^2} \\ &= 1.2 \times 10^{-3} \text{ sr}. \end{aligned} \quad (4)$$

Our cylindrical samples were aluminum tubing of nominally 152 mm outside diameter; the spheres were spun copper, with a diameter of nominally 203 mm. The size of each sample was measured in the image plane, and camera parameters were adjusted from the size and position of the image in the primary camera.

#### D. Data Processing

The data that result from the measurement of a single BRDF are

- 32 measurement images from the primary camera (or 96 when three filters are used for RGB), with a record of the lens aperture and neutral-density filter used for each; and
- 32 light source calibration images from the secondary camera.

The major steps involved in processing these data are

1. Use the targets visible in the calibration images to establish the poses of the secondary camera, and from them compute the light source positions.
2. Find the image of the test sample in one of the photographs from the primary camera, and use its size and position to determine the sample's position.
3. Sample the images to obtain measurements covering part or all of the surface's BRDF.

The first step is performed by fully automatic software, which locates targets in each secondary camera image and calculates camera poses. The targets in each calibration image are used as input to a nonlinear fitting procedure that solves for the camera pose by minimizing the image-space discrepancy between the projections of the targets' known 3-D positions and their measured locations in the image.

The only human intervention required is in the second step, where the user clicks on a number of points along the boundary of the sample in one measurement image; these points are used to allow sub-pixel precision in the determination of the position and size of the sample's image.

The final step works by ray tracing: For each pixel in the primary camera image, the corresponding surface point and normal are determined, then the direction of illumination is computed. The relative irradiance is computed from the known source geometry; then the relative value of the BRDF is computed by division of the pixel value, which is proportional to radiance, by the irradiance. All that remains is to normalize this relative value to the measured and known BRDF value of our reference sample. This computation can be carried out once per pixel to obtain a scattered set of raw samples, which will fall on a set of 2-D surfaces, or sheets, in the 3-D domain of the BRDF.

The generation of BRDF values at arbitrary points requires the reconstruction of a full 3-D function. Where such arbitrary evaluation was necessary for the figures in this paper, we employed a local quadratic regression procedure,<sup>18</sup> using an elliptical kernel to span the distances between the sheets defined by individual images without unnecessarily blurring the data along the sheets.

#### 4. Verification

To verify the technique, we began with a cylindrical sample, which allowed measurement of BRDF in the incidence plane. This type of measurement provided simpler data for verification and analysis before we moved on to measuring the full BRDF. It also allowed us to average several scan lines to reduce noise. We also measured flat samples of each material independently, using a gonireflectometer that was designed and verified for accuracy within 5%.<sup>19</sup> We validated the image-based measurements both by verifying reciprocity and by comparing the data from the two independent measurement systems. The new method gives results comparable in accuracy to the gonireflectometer: Consistency is excellent out to 75° incidence (or exitance) and reasonable out to approximately 85°.

We measured a piece of ordinary photocopy paper (Xerox 4200DP, 20 lb.) by wrapping it around a cylinder. The resulting measurements fall on a planar slice of the BRDF, yielding a function of two angles:  $\rho_{bd}(\theta_i, \theta_e)$ . In Fig. 9, we plot the data as a height field over the  $(\theta_i, \theta_e)$  plane; each curve contains the data from a single image. The dense sampling of our method yields over 4000 points even for this small

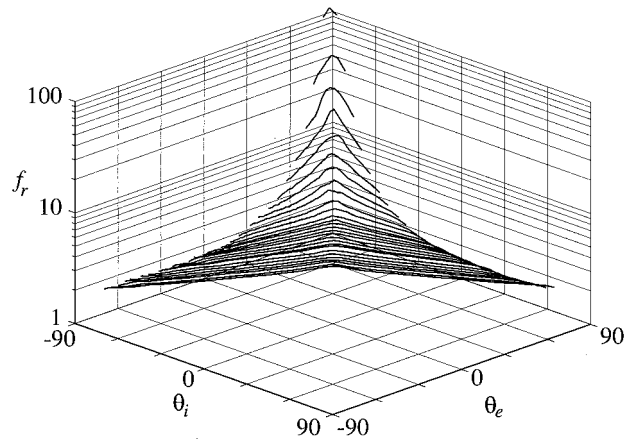


Fig. 9. Incidence-plane BRDF measurements plotted against incident and exitant angles.

subset of the total BRDF. Even for such a diffuse surface, we see noticeable directional variation; the graph of an ideal Lambertian surface would be a flat plane. Reciprocity demands that the plot be symmetric left to right, providing an initial check on the data.

We further check our measurements quantitatively, both for reciprocity and by comparing against an instrument of known accuracy. Reciprocity can be evaluated from Fig. 10, in which the dashed curves show the data for three fixed values of  $\theta_i$  and the solid curves show the data for fixed  $\theta_e$ . Each pair of curves represents two independent measurements: The data are measured from different parts of the surface, except in the specular direction. Note the close correlation for all angles up to 85°. The rms deviation over all data out to 75° is 1.5%, and data out to 85° still satisfy reciprocity to within 6%. The error figures reported in this paper are the rms average of the relative error between the two sets of data, after linear interpolation to match the sample patterns. Figure 11 compares the data from the image-based measurements with independently measured data from the gonireflectometer. The discrepan-

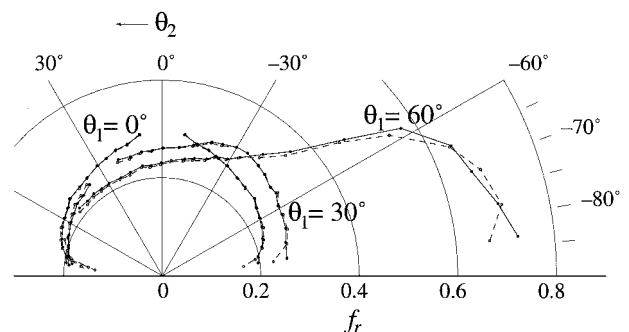


Fig. 10. Reciprocity comparison for white paper. BRDF measurements plotted for three fixed incident and exitant angles. Dashed curves are the fixed incident angles; solid curves are fixed exitant angles.

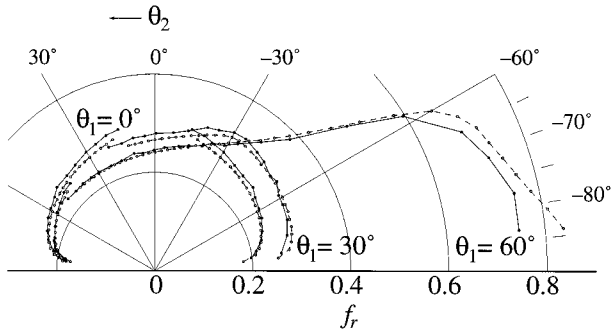


Fig. 11. Gonioreflectometer comparison for white paper. Image-based BRDF measurements (solid curves) and gonioreflectometer measurements of the same material (dashed curves).

cies between the two systems are 2.8% (to 75°) and 3.7% (to 85°).

We also measured a flat gray primer; this surface shows greater deviation from a Lambertian BRDF, generating a much greater dynamic range. A reciprocity comparison is shown in Fig. 12; the data are plotted at two scales to show the entire range of magnitudes. Reciprocity held within 2.5% to 75° and within 7.8% to 85°.

### 5. Results

We used the system described above to measure the full isotropic BRDF of three paints, shown photographed in Fig. 13. These are a gray primer, a blue enamel, and a red metallic automotive lacquer. The

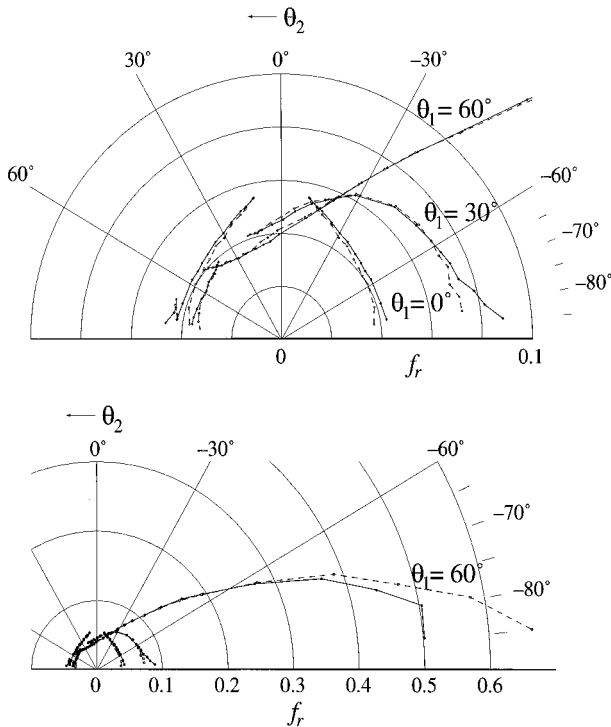


Fig. 12. Reciprocity comparison for gray primer. BRDF measurements are plotted for three fixed incident and exitant angles. Dashed curves are fixed incident angles; solid curves are fixed exitant angles.



Fig. 13. Photographs of actual test samples used.

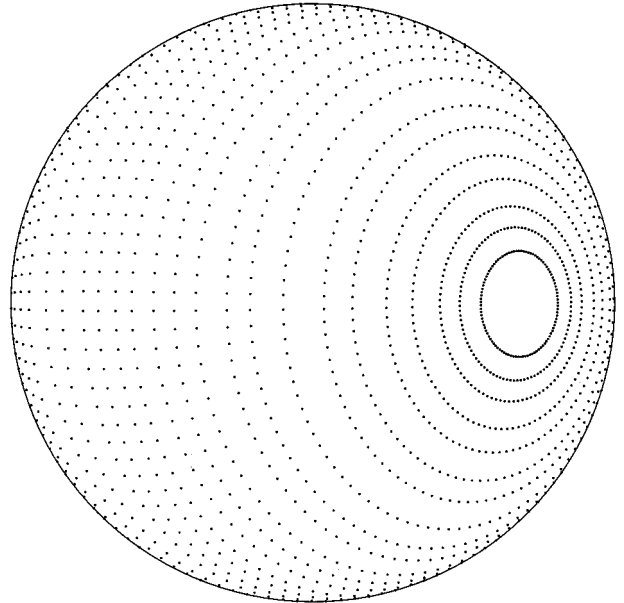


Fig. 14. BRDF sampling pattern for a single incident direction. Each ring is derived from a single digital image.

red and blue paints were coated with a gloss-reducing finish. For the two colored paints we used RGB color separation filters, and for the primer we made a single broadband measurement. The data for each color channel of each BRDF comprise some 1.5 million samples; approximately 6000 of these, corre-

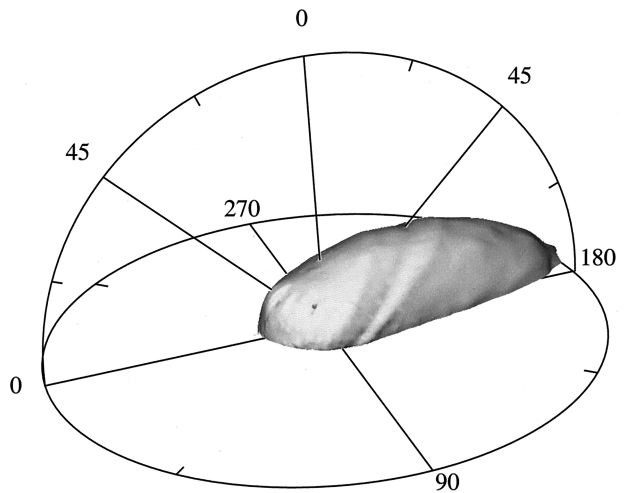


Fig. 15. Scattering diagram for the gray primer at  $\theta = 45^\circ$ . The scale is double that used for the red and blue paints.

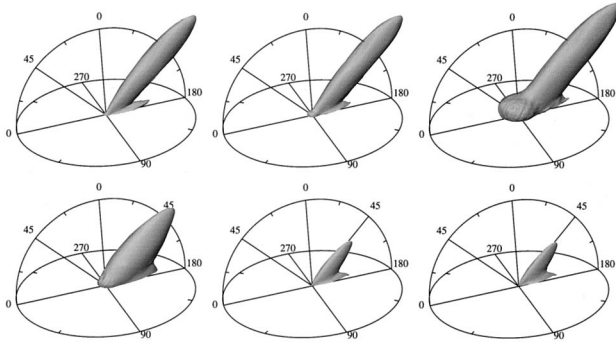


Fig. 16. Resampled scattering diagrams of the BRDF measurements of two paints: a blue enamel (top row) and a red automotive lacquer (bottom row). The RGB color measurements are shown from left to right.

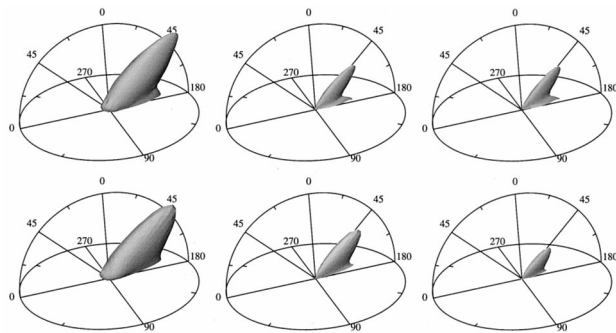


Fig. 17. Image-based measurements of the red paint (top row; identical to bottom row of Fig. 16) with the corresponding measurements from the gonioreflectometer (bottom row). The gonioreflectometer data were triangulated directly from the sample points, whereas the image-based data, which do not come in sets of fixed  $\theta$ , were resampled.

sponding to a single exitant angle, are plotted in Fig. 14. Each ring of points is extracted from a single measurement image.

Figure 15 shows a 3-D scattering diagram of the primer for an incident angle of  $45^\circ$ . The surface is clearly non-Lambertian, showing a broad forward-scattering peak. Figure 16 shows similar plots for the RGB wavelength bands of the two colored paints.

We measured the red paint with the gonioreflectometer to validate our results over the entire hemisphere. Figure 17 shows the gonioreflectometer measurements alongside the image-based measurements from Fig. 16. These plots indicate that our technique has successfully captured the BRDF. The differences in red and blue channels are accounted for, we believe, by the different wavelength ranges of the two instruments; the CCD camera's sensitivity extends beyond the gonioreflectometer's limit of  $\approx 710$  nm, and our system's signal-to-noise ratio is far superior below approximately 450 nm.

## 6. Conclusions and Future Work

We have described a simple technique that can exhaustively measure the BRDF of many materials

with general-purpose equipment. We achieve accuracy rivaling that of a specialized gonioreflectometer but with much greater speed and angular resolution. The technique is rapid because the two dimensions of a camera image sample two angular degrees of freedom instantaneously, leaving only one to be handled by sequential measurement. Our system can acquire 1.5 million monochrome samples covering an entire isotropic BRDF in less time than it takes to prepare a test sample. The resulting data are internally consistent and agree closely with independent measurements.

Our technique is limited to measurement of curved surfaces with uniform BRDF's. To measure the full hemispherical BRDF, we must apply the finish to a compound-curved surface by spraying, dipping, grinding, etc., but we can also measure the incidence-plane reflectance of any material that can be wrapped around a cylinder.

We have demonstrated measurements of isotropic BRDF's, but the technique can also be extended to measure the BRDF of an anisotropic surface. To do this, we must rotate the sample to provide a fourth degree of freedom. Either a spherical sample with uniform anisotropic BRDF and known orientation can be used or anisotropic samples of flat, flexible materials can be measured in the plane of incidence when the sample is rotated on the cylinder to achieve different values of  $\phi$ .

We also plan to extend our technique to glossier surfaces. Our detector handles a dynamic range of the order of 3.5 orders of magnitude, so we applied a low-gloss finish to the colored paints to simplify this initial demonstration of the technique. We can extend our dynamic range by making multiple exposures through different neutral-density filters and combining them as did Debevec and Malik.<sup>20</sup> As we measure glossier surfaces, we will also have to account for the finite solid angles of source and detector.

This method already uses equipment much less expensive than a traditional gonioreflectometer (the gonioreflectometer used for validation cost more than four times as much as the equipment used for our image-based measurements), but the cost of our setup could be reduced even further.

- A simpler secondary camera could be used; color is unneeded, and lower resolution would still locate the light source with sufficient accuracy. Several consumer CCD camera models should be adaptable for this purpose.
- A less expensive primary camera could be used, but the higher noise of such a camera would reduce dynamic range. Multiple-exposure techniques could recover some dynamic range, but would ultimately be limited by blooming in the CCD and optical flare.

The authors were supported by the National Science Foundation (NSF) Science and Technology Center for Computer Graphics and Scientific Visualization (ASC-8920219) and by NSF grant ASC-9523483. S. R. Marschner was also partly sup-



ported by the Hewlett-Packard Corporation, who also donated several of the workstations used in this research. Measurement equipment was provided by NSF grant CTS-9213183 and by a donation from the Imaging Science Division of the Eastman Kodak Company.

## References

1. F. E. Nicodemus, J. C. Richmond, J. J. Hsia, I. W. Ginsberg, and T. Limperis, "Geometric considerations and nomenclature for reflectance," Natl. Bur. Stand. (U.S.) Monogr. **160** (U.S. Department of Commerce, Washington, D.C., 1977).
2. J. F. Blinn, "Models of light reflection for computer synthesized pictures," Comput. Graph. **11**, 192–198 (1977).
3. K. E. Torrance and E. M. Sparrow, "Theory for off-specular reflection from roughened surfaces," J. Opt. Soc. Am. **57**, 1105–1114 (1967).
4. G. J. Ward, "Measuring and modeling anisotropic reflection," Comput. Graph. **26**, 265–272 (1992).
5. American Society for Testing and Materials, *Standard Practice for Angle Resolved Optical Scatter Measurements on Specular or Diffuse Surfaces* (American Society for Testing and Materials, West Conshohocken, Pa., 1996), Standard E 1392–96.
6. K. E. Torrance and E. M. Sparrow, "Off-specular peaks in the directional distribution of reflected thermal radiation," ASME J. Heat Transfer **88**, 223–230 (1966).
7. R. J. Castonguay, "New generation high-speed high-resolution hemispherical scatterometer," in *Optical Scattering: Applications, Measurements, and Theory II*, J. C. Stover, ed., Proc. SPIE **1995**, 152–165 (1993).
8. Z. R. Hatab, J. R. McNeil, and S. S. H. Naqvi, "Sixteen-megabit dynamic random access memory trench depth characterization using two-dimensional diffraction analysis," J. Vac. Sci. Technol. B **13**, 174–181 (1995).
9. J. R. McNeil and S. R. Wilson, "Two-dimensional optical scatterometer apparatus and process," U.S. patent 5,241,369 (31 August 1993).
10. K. J. Davis and D. C. Rawlings, "Directional reflectometer for measuring optical bidirectional reflectance," U.S. patent 5,637,873 (10 June 1997).
11. K. Ikeuchi and K. Sato, "Determining reflectance properties of an object using range and brightness image," IEEE Trans. Pattern Anal. Mach. Intell. **13**, 1139–1153 (1991).
12. R. Lu, J. J. Koenderink, and A. M. L. Kappers, "Optical properties (BRDF) of velvet," Appl. Opt. **37**, 5974–5984 (1998).
13. G. C. Holst, *CCD Arrays, Cameras, and Displays* (SPIE, Bellingham, Wash., 1996).
14. S. S.-F. Chen, J. W.-C. Li, K. E. Torrance, and S. N. Pattanaik, "Preliminary calibration of the photometrics PXL1300L CCD camera," Technical Report PCG-96-1 (Cornell University Program of Computer Graphics, Ithaca, N.Y., 1996).
15. S. N. Pattanaik and K. E. Torrance, "Light measurement using the photometrics PXL1300L CCD camera," Technical Report PCG-98-1 (Cornell University Program of Computer Graphics, Ithaca, N.Y., 1998).
16. C. S. Fraser, M. R. Shortis, and G. Ganci, "Multi-sensor system self-calibration," in *Videometrics IV*, S. F. El-Hakim, ed., Proc. SPIE **2598**, 2–18 (1995).
17. J. H. Chandler and C. J. Padfield, "Automated digital photogrammetry on a shoestring," Photogramm. Rec. **15**, 545–559 (1996).
18. J. Fan and I. Gijbels, *Local Polynomial Modeling and Its Applications* (Chapman & Hall, London, 1996).
19. S. C. Foo, "A gonioreflectometer for measuring the bidirectional reflectance of material for use in illumination computation," M.S. thesis (Cornell University, Ithaca, N.Y., 1997).
20. P. E. Debevec and J. Malik, "Recovering high dynamic range radiance maps from photographs," Comp. Graph. Proc., Annual Conference Series, 369–378 (1997).